Multi-Sectional Lift Actuation for Wind Turbine Load Alleviation

Multi-Sectional Lift Actuation for Wind Turbine Load Alleviation

Chang Liu, Abhineet Gupta, Mario Rotea
UTD Center for Wind Energy
The University of Texas at Dallas, Richardson, TX 75080, USA

E-mail: rotea@utdallas.edu

Abstract. The development of large rotors can be limited by the ability to manage dynamic loads. Active Flow Control (AFC) actuators have been proposed to reduce these dynamic loads. This paper aims to study and quantify the advantages of using multiple AFC actuators compared to using a single AFC actuator for each blade. For this study, AFC actuators are idealized and modeled as instantaneous changes to the local lift coefficient at the corresponding blade sections. We refer to this idealized actuators as sectional lift actuators (SLA). A comparison between a single SLA and two SLAs per blade is made using feedforward and feedback control. Blade loads in above-rated wind conditions are used for the comparative analysis, which is conducted using the DTU-10MW reference turbine model.

1. Introduction

Wind turbines are progressively moving toward larger rotor diameters to lower the 'Levelized Cost of Energy' (LCOE) by increasing the annual energy production. The practical realization of large rotors can be limited by the ability to manage dynamic loads on the wind turbine. These dynamic loads are generated due to gravity, tower shadow, wind shear/veer, unsteady turbulent wind and other sources like wind gusts [1]. Therefore, controlling these dynamic loads is required to realize the benefits of ultra large wind turbine rotors.

Various techniques have been implemented for controlling the dynamic loads on the wind turbine. 'Individual Pitch Control' (IPC) has been studied widely and has been shown to reduce fatigue loads for small to medium size turbines [2, 3]. For turbines with large rotors, IPC may be hampered by the need for fast and robust actuators, the risk of excessive wear of the pitch actuators and a limited ability for localized control action along the blade span. Due to these limitations of IPC, Active Flow Control (AFC) devices have been proposed and evaluated [4]. These AFC devices include trailing edge flaps, microtabs, vortex generators and plasma actuators. The advantage of these AFC devices is that they offer fast and local control authority which can facilitate load control at higher temporal and spatial resolutions as compared to IPC. AFC devices are especially beneficial for long and flexible blades as they provide for faster load control actuation and localized control abilities.

This paper is a first step toward answering the following research question: *What advantages, if any, result from using multiple AFC devices as compared to using a single AFC device on each blade to reduce dynamic loads?*

To answer this question, the AFC actuator is idealized as an actuator that can modify the local lift coefficient of a chosen section of the turbine blade. This idealized actuator is called

a 'sectional-lift actuator' (SLA). The load reduction performance of multiple (two) SLAs is compared with the performance of a single SLA. The main evaluation criteria for the comparison are the flapwise bending moments at the blade root. Secondary evaluation criteria include moments at the tower base, edge-wise blade root bending moments and the low-speed shaft torsional moment. The comparison is made for above-rated wind conditions. These studies are conducted using the FAST model DTU-10MW reference turbine [5] with the basic DTU turbine controller [7] implemented in the simulation software SIMULINK. The comparison between single and multiple SLAs is made using both feedforward and feedback control.

2. Methodology

In order to study dynamic load control using single and multiple SLAs, the NREL FAST v8.16.00a [6] model of DTU-10MW wind turbine is utilized. The FAST model of the turbine is modified to implement and simulate the SLAs on the turbine blade. This modeling methodology has been introduced in [8] and illustrated with a simple control design. Key parameters for the turbine are summarized in Table 1. The SIMULINK version of the published DTU controller [7], which is a 'variable-speed, collective-pitch' controller, is implemented as the turbine controller.

Table 1. Properties of DTU-10MW turbine model

Parameter	Value
Rated Power	10 MW
Rotor Diameter	178.3 m
Hub Height	119.0 m
Cut-in, Rated, Cut-out Wind Speed	4 m/s, 11.4 m/s, 25 m/s
Cut-in, Rated Rotor Speed	6 rpm, 9.6 rpm

SLAs are modeled with AeroDyn v14. It is assumed that the actuator is capable of changing the lift coefficient within a range of $\Delta C_L = \pm 0.2$ compared to the baseline lift coefficient at the specific blade span section. The baseline and actuated lift coefficient curves are shown in Fig. 1.

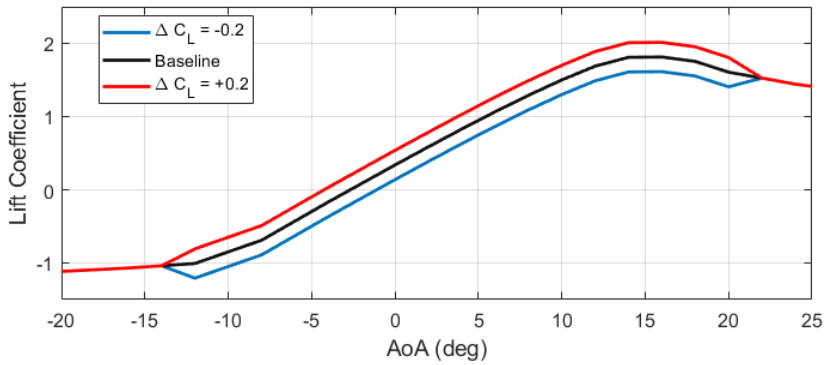

Figure 1. Baseline (black line) and actuated lift coefficient curves.

For this study, two sectional lift actuators are implemented on each blade of the wind turbine. Figure 2 shows the aerodynamic elements of the blade used to model the aerodynamic forces on the wind turbine by FAST. There are 37 aerodynamic elements in each blade. SLAs are implemented on elements numbered 24 to 37 with a total length of 26.7 meters. The SLAs cover approximately 30% of the blade span. For single SLA, this entire length of the blade is considered to be one section. For two SLAs, blade elements 24 to 28, with a total span of 12.8 meters, are defined as section-1 (inner section) and blade elements 29 to 37, with a span of 13.9 meters, are defined as section-2 (outer section).

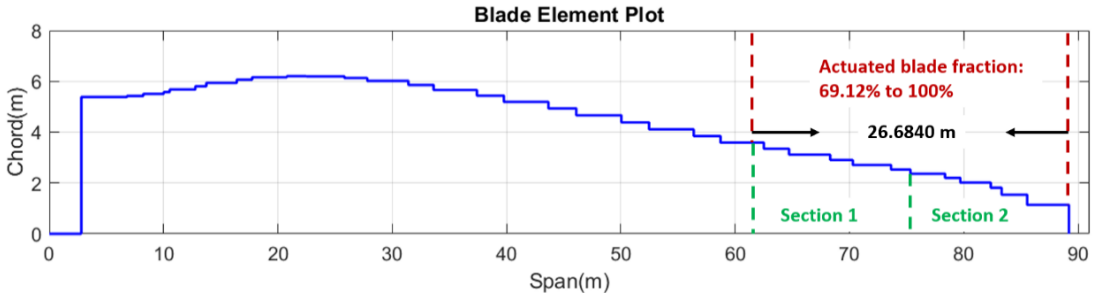

Figure 2. Blade element plot of DTU-10MW turbine.

The FAST model of the turbine is a nonlinear simulation model which is not suitable for control design. Therefore, in order to design dynamic load controllers, the system is linearized to obtain a linear state space model of the turbine. Computing software MATLAB is utilized for this purpose. Specifically, the Prediction-Error Minimization (PEM) algorithm provided by the system identification toolbox of MATLAB is employed. Further details of the system identification process are described in Section 3.

Two dynamic load control architectures are designed and implemented, and the performance of single SLA and multiple SLAs are compared for each case. The first control architecture is a feedforward design which commands the sectional-lift based on the current azimuth angle of the rotor calculated using the rotor speed. This control system is described in detail in Section 4.1. The second architecture is a feedback control design which measures the flapwise root bending moment and commands the sectional lift control signal based on the measurements. This control system and resulting analysis are described in Section 4.2.

3. Linear Model for Control System Design

In order to design the dynamic load control system, Multi-Blade Coordinate transformations (MBC) [9] are utilized. It is assumed that the 3 blades are identical and 120 degrees apart. Therefore, the MBC can be utilized to extract one-per-revolution (1P) harmonic loads from the blade root sensors. MBC uses the azimuth angle (θ) of the rotor for the calculation of harmonic loads. Figure 3 shows the implementation of MBC on the turbine model. Forward MBC is used to transform the flapwise root bending moments of the three blades (M_1, M_2, M_3) from the rotating frame to fixed frame (M_{cos}, M_{sin}). Thus, essentially the 1P harmonic loads in the rotating frame are transformed into constant loads in fixed frame. The forward MBC transformation can be written as follows:

$$\begin{bmatrix} M_{cos} \\ M_{sin} \end{bmatrix} = \frac{2}{3} \begin{bmatrix} \cos\theta & \cos\left(\theta + \frac{2\pi}{3}\right) & \cos\left(\theta + \frac{4\pi}{3}\right) \\ \sin\theta & \sin\left(\theta + \frac{2\pi}{3}\right) & \sin\left(\theta + \frac{4\pi}{3}\right) \end{bmatrix} \begin{bmatrix} M_1 \\ M_2 \\ M_3 \end{bmatrix} \tag{1}$$

where θ is the azimuth angle (in radians) of the turbine rotor. The right inverse of this MBC transformation can be utilized to command the sectional-lift actuator signal on the three blades

(u_1, u_2, u_3) by transforming the corresponding signals in the fixed frame (u_{cos}, u_{sin}). This is shown as the Inverse MBC block in Fig. 3. The Inverse MBC transformation can be written as follows:

$$\begin{bmatrix} u_1 \\ u_2 \\ u_3 \end{bmatrix} = \begin{bmatrix} \cos\theta & \sin\theta \\ \cos\left(\theta + \frac{2\pi}{3}\right) & \sin\left(\theta + \frac{2\pi}{3}\right) \\ \cos\left(\theta + \frac{4\pi}{3}\right) & \sin\left(\theta + \frac{4\pi}{3}\right) \end{bmatrix} \begin{bmatrix} u_{cos} \\ u_{sin} \end{bmatrix} \tag{2}$$

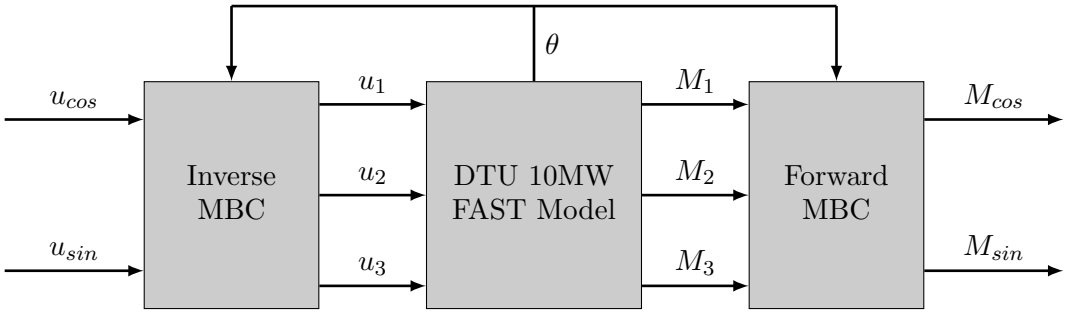

Figure 3. Block diagram of wind turbine with MBC transformations.

In order to design the dynamic load control, 2×2 linear systems, denoted by G hereafter, are identified in fixed frame. The inputs of the linear system are the nondimensional u_{cos} and u_{sin} and the outputs are M_{cos} and M_{sin} (in kN·m). MATLAB is utilized to perform the system identification. Two Pseudo-Random Binary Signals of 2000 seconds are generated and passed through a low pass filter to obtain the excitation signals for system identification. These signals are then used to excite the system at the inputs u_{cos} and u_{sin}. The two outputs M_{cos} and M_{sin} are logged. This time domain data is used to identify a linear state space model in the fixed frame using the Prediction-Error Minimization (PEM) algorithm. The system identification process is performed for both single SLA and multiple SLAs.

Figure 4 shows the bode plot for the identified system with single SLA. The figure also shows the 1P frequency at rated rotor speed with a red line. This frequency is highlighted since the feedback controllers are designed with approximately 1P closed loop bandwidth. The frequency responses are relatively flat in this bandwidth with little to no phase lag. This implies the plant has relatively simple dynamics in the bandwidth of interest, which facilitates the design of feedback controllers. Similar behavior is observed for the system with multiple SLAs; the transfer functions are omitted due to space limitations.

4. Dynamic Load Control

To study the potential advantages of multiple sectional-lift actuators, load control systems with single SLA and multiple SLAs are implemented. Two different control architectures are considered and analyzed to draw relevant conclusions. These architectures are described in Section 4.1 and Section 4.2.

4.1. Feedforward Control

A feedforward dynamic load control system is implemented and analyzed with two sections per blade. For this controller, the dynamic loads are not measured and only the instantaneous azimuth angle (θ) is used to decide the sectional-lift signals. The azimuth angle can be calculated using the rotor speed as $\theta = \int \omega \, dt$.

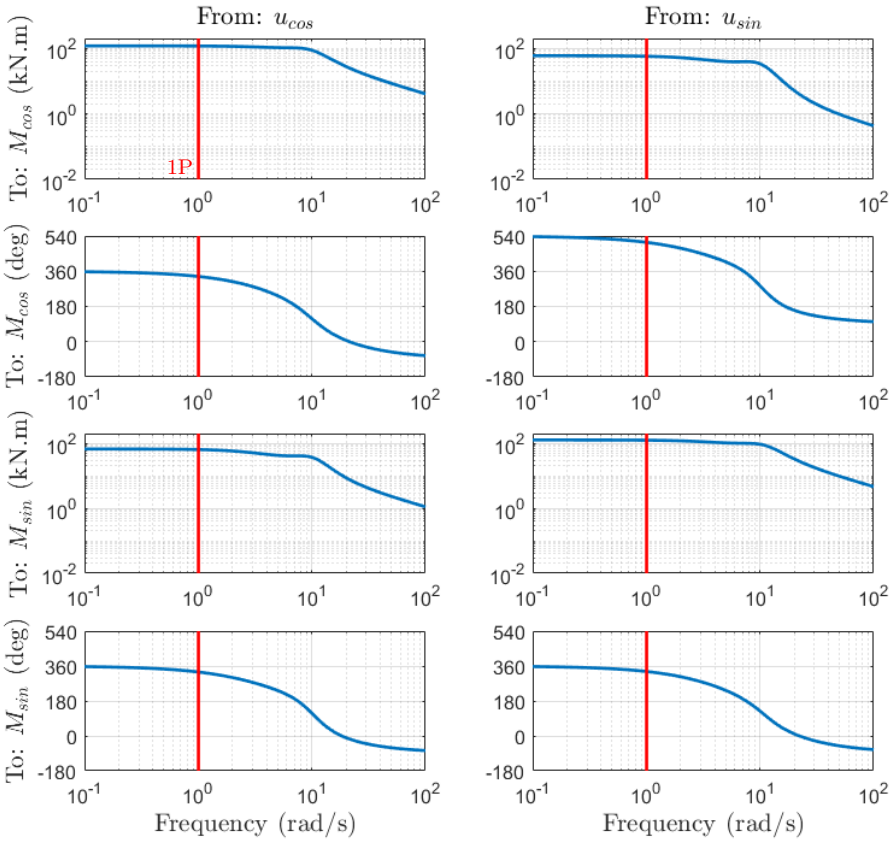

Figure 4. Bode plot of identified system with single SLA.

The control signals to the two SLAs on the blades calculated by the feedforward controller are given in Eqn. 3, where $u_{i,j}$ is the sectional lift command to the j^{th} SLA on the i^{th} blade and ϕ_1 and ϕ_2 are the inner and outer phase offset angles. The amplitudes of the sectional lift commands are chosen to be the maximum ΔC_L achievable by the SLA (0.2) as shown in Fig. 1. The optimal phase offset angles ϕ_1 and ϕ_2 are determined by evaluating damage equivalent loads using an exhaustive search over the phase angles.

$$
\begin{aligned}
u_{1,1} &= 0.2 \times \sin\left(\int \omega\, dt + \phi_1\right) & u_{1,2} &= 0.2 \times \sin\left(\int \omega\, dt + \phi_2\right) \\
u_{2,1} &= 0.2 \times \sin\left(\int \omega\, dt + \frac{2\pi}{3} + \phi_1\right) & u_{2,2} &= 0.2 \times \sin\left(\int \omega\, dt + \frac{2\pi}{3} + \phi_2\right) \\
u_{3,1} &= 0.2 \times \sin\left(\int \omega\, dt + \frac{4\pi}{3} + \phi_1\right) & u_{3,2} &= 0.2 \times \sin\left(\int \omega\, dt + \frac{4\pi}{3} + \phi_2\right)
\end{aligned} \tag{3}
$$

Simulations are conducted at 'above rated' wind speed with vertical shear and no turbulence. The mean wind speed at hub height is chosen to be 18 m/s and the shear exponent is chosen to be $\alpha = 0.2$. The reductions in flapwise blade root moment are evaluated as a function of the control signals phase offset angles (ϕ_1 and ϕ_2). The metric for this analysis is the Damage Equivalent Load (DEL) of the time domain flapwise root bending moment signal. The DELs are normalized by the DEL of the blade root bending moment with no sectional-lift control. Thus, a unitary normalized DEL corresponds to the baseline turbine with no feedforward load control. A lower value of normalized DEL indicates a reduction of dynamic loads. The normalized DEL

is defined by:

$$\mathrm{DEL}_N = \frac{\mathrm{DEL}_{(SLC\ ON)}}{\mathrm{DEL}_{(SLC\ OFF)}} \tag{4}$$

Figure 5 shows the contour plot of DEL_N for a range of phase offset angles (ϕ_1 and ϕ_2). The results for blade 1 are shown; the other two blades have similar responses since the flow is steady, albeit nonuniform. The plot on the left shows that lower DELs (higher load reductions) appear in the lower-left corner of the graph. A contour plot with finer resolution for this region is shown on the right. The lowest (optimal) normalized DEL is observed to be around $\phi_1 = -120$ deg and $\phi_2 = -115$ deg. The optimal normalized DEL is $\mathrm{DEL}_N = 0.75$, which represents a load reduction of 25%. This is shown as a black cross in Fig. 5. If both phase offset angles are equal to -120 deg, the normalized DEL remains virtually the same as shown with the orange cross in the figure.

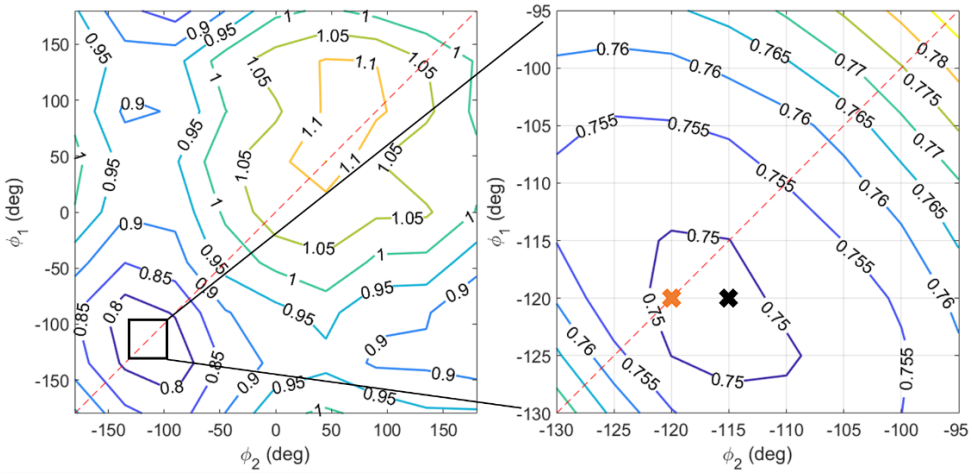

Figure 5. Contour plot of normalized DEL w.r.t phase offset angles for blade #1.

The significance of the result in Fig. 5 can be understood by taking a closer look at the control signals described in Eqn. 3. It is clear from the equation that as the optimal phase shift angles ϕ_1 and ϕ_2 are equal, the command signals to the two sections are the same and thus, they behave as a single section, which can be controlled with a single sectional lift command.

4.2. Feedback Control

Next, a feedback controller is designed and implemented to compare load control using a single SLA and multiple SLAs. The objective of the feedback control is to reduce the 1P harmonic (and neighboring frequencies) of the flapwise blade root bending moment in the rotating frame. The forward MBC transformation shifts the 1P harmonic load in the rotating frame to 0P in the fixed frame [10]. This implies that the dynamic load control problem can be posed as a disturbance rejection problem in the fixed frame, from zero frequency to a given bandwidth ω_0. In this paper we take $\omega_0 = 0.8$P.

The controller measures the flapwise root bending moment and commands the sectional-lift control signals. The block diagram of the feedback control architecture is shown in Fig. 6. The block F represents a nonlinear map to handle actuator saturation and integrator anti-windup and the block K represents a linear controller designed using robust control theory. The actual implementation of F and K remains proprietary and cannot be disclosed at this time. The

frequency ω_0 is taken to be 0.8P and is approximately the crossover frequency of magnitude of the multivariable loop transfer function $L(s)$ defined by:

$$L(s) = G(s) \times \frac{\omega_0}{s} \times K(s) \tag{5}$$

where G is linear model identified by system identification. The frequency ω_o is approximately the bandwidth of the closed loop system.

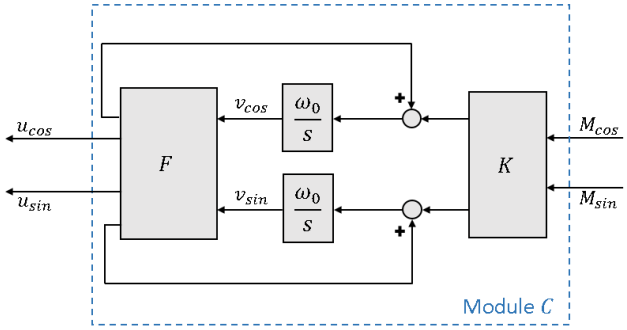

Figure 6. Architecture of the feedback controller module.

To illustrate the design method, the case of a single SLA and multiple SLAs are considered and the results are compared. The controllers are designed for 18 m/s steady mean wind speed. Figure 7 describes the implementation of the feedback controller with a single SLA where the control module C is shown in Fig. 6. Similarly, Fig. 8 describes the implementation of the feedback controller with multiple SLAs. In the figure, $u_{i,j}$ is the sectional lift command to the j^{th} SLA on the i^{th} blade. The control modules C_1 and C_2 have the architecture shown in Fig. 6.

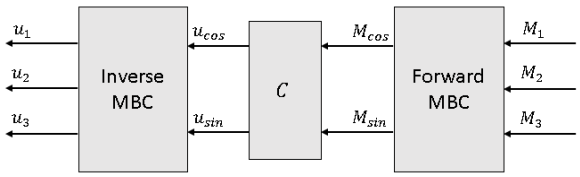

Figure 7. Feedback load control using single SLA.

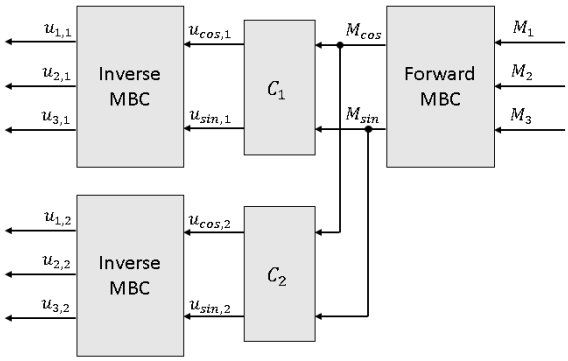

Figure 8. Feedback load control using multiple SLAs.

The feedback controller is first analyzed with the same wind conditions as the feedforward controller; i.e., a mean wind speed at hub height of 18 m/s and shear exponent $\alpha = 0.2$. The time domain responses of feedback control with single SLA are shown in Fig. 9, where the plot on the top shows actuator commands and the plot below shows the flapwise root bending moments. The feeback controller is activated at 250 sec. The flapwise root bending moments are also shown in the frequency domain in the bottom plot. The 1P, 2P and 3P frequencies

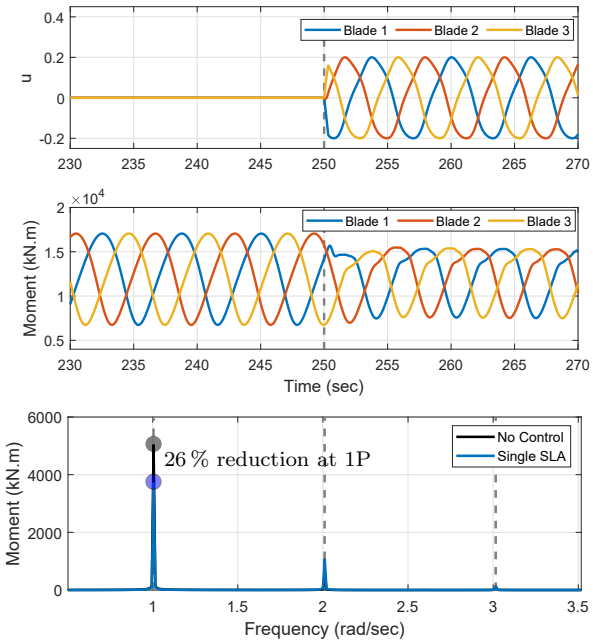

Figure 9. Response from feedback control with single SLA.

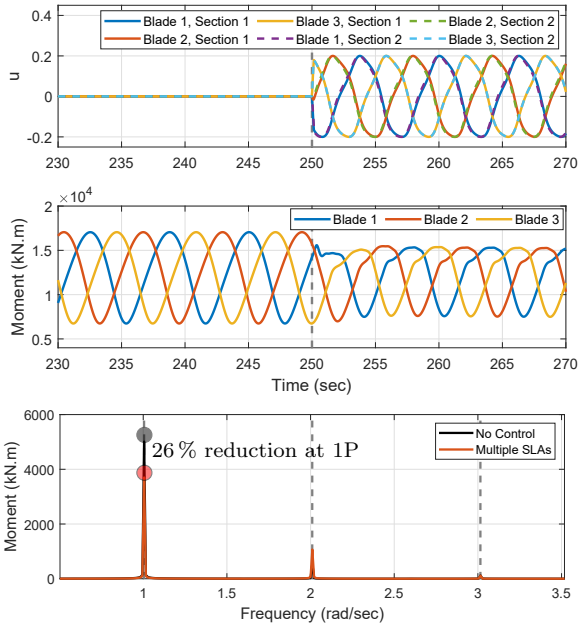

Figure 10. Response from feedback control with multiple SLAs.

have been highlighted in the frequency domain plots with gray lines. Similarly, Fig. 10 shows the response with multiple SLAs.

The single SLA and the two-SLA feedback controllers deliver similar performance. The controllers reduce the 1P harmonic load by 26% as shown in the bottom plots in Figs. 9 and 10. The normalized damage equivalent loads have been calculated using Eqn. 4. The results are essentially the same as the optimal feedforward case: *the DEL reduction with feedback control on one or two sections is* 25% *approximately (cf. Fig. 5).*

A more detailed comparison between the single SLA and multiple SLAs cases has been performed using DEL calculations with shear and turbulence. Simulations are conducted following IEC 61400-1 standard design load case (DLC) 1.2 [11] for three wind mean speeds at 'above rated' conditions (15 m/s, 18 m/s, and 21 m/s). The feedback controllers are the ones designed for 18 m/s; i.e., controllers are not scheduled with wind speed. Turbulent wind files of a duration of 600 seconds are generated using TurbSim with six different random seeds. The load reduction capabilities of the feedback controller with single SLA and multiple SLAs are determined by evaluating the DELs calculated with MLife [12].

Normalized DELs are calculated for the flapwise blade root bending moments as well as key loads such as edgewise blade root bending moments, tower fore-aft (FA), tower side-to-side (SS), and low-speed shaft (LSS) torsional moments. Normalized DELs are obtained using Eqn. 4.

Figure 11 shows the normalized DELs for feedback control. No significant difference is observed between single SLA and multiple SLAs. This is true for both the controlled flapwise root bending moments and other loads (tower, blade edgewise, low-speed shaft torsion). For the flapwise bending moment, which is the controlled moment, any DEL differences could be attributed to factors such as statistical variations in the load time series, and/or the fact that controllers are designed for the 18 m/s model and evaluated at off-design speeds of 15 m/s and 21 m/s. *Thus, from this study, it follows that multiple SLAs do not provide benefits in terms of load reduction as compared to single SLA.*

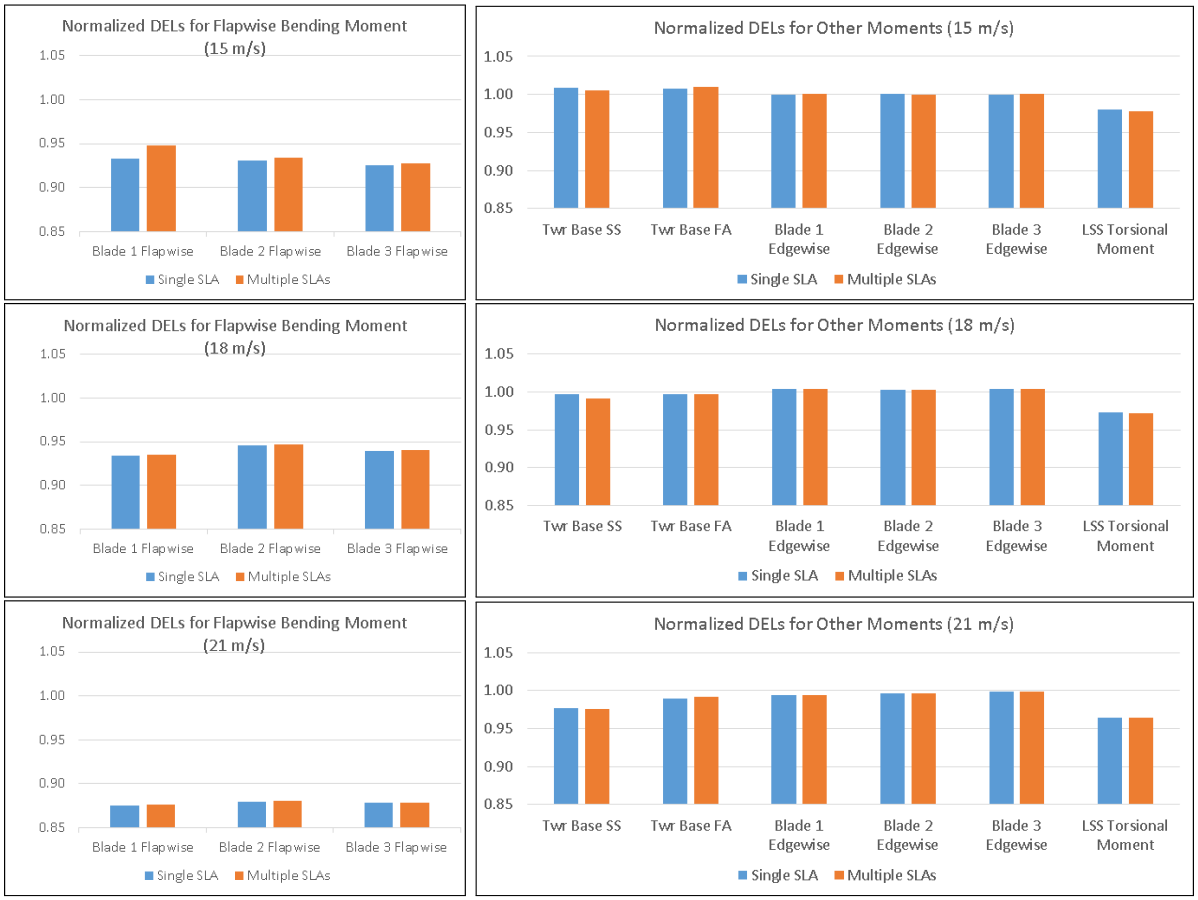

Figure 11. Performance of feedback sectional lift controllers for above-rated wind conditions.

To obtain a full picture of the effect of the sectional lift controllers, we evaluate turbine performance. More specifically, we calculate the normalized root mean square values (RMS) of speed error, power error and pitch rate. The speed and power errors are obtained by subtracting the corresponding rated values from the rotor speed and power. The RMS of these error signals are calculated and then normalized by the corresponding rated values. For pitch rate, the RMS of the pitch rate signal is calculated and normalized by the maximum allowable pitch rate. Figure 12 shows normalized RMS values for rotor speed error, power error and pitch rate for the turbine with no control (grey bars) and feedback control with single (blue bars) and multiple SLAs (orange bars). It can be seen that feedback controllers with both single SLA and multiple SLAs do not affect the turbine performance in any significant way as compared to no sectional lift control. The fact that the pitch activity does not increase when lift control is active is an advantage over IPC, as the latter requires an increase in pitch activity to reduce blade loads.

5. Conclusion

The aim of this work is to compare single versus multiple SLAs for dynamic load control of wind turbines. Both feedback and feedforward controls are implemented to drive the SLAs. No differences, between single and multiple SLAs, are observed in the primary dynamic loads (flapwise blade root bending moments). A similar statement can be made for the secondary loads (edgewise blade root bending moments, tower moments, etc). *Thus, from this limited study, it can be concluded that multiple SLAs do not yield load reduction gains over a single*

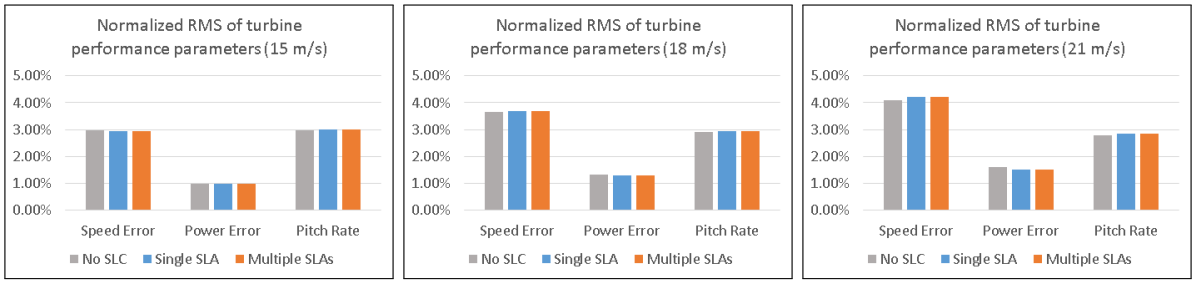

Figure 12. Effect of feedback sectional lift control on turbine performance for above-rated wind conditions.

SLA of the same combined size and location. However, this conclusion may not remain valid if one or more of the following assumptions do not hold true:

- The feedforward controller in Eqn. 3 is a sinusoidal waveform of 1P frequency.
- The feedback controller module C in Fig. 6 is designed for a closed loop bandwidth not exceeding 1P.
- The feedback controllers use a first-order (1P) MBC transformation framework to calculate sectional lift commands as shown in Figs. 7 and 8.

Understanding the impact of violating one or more of these assumptions is outside the scope of this paper and left for future work.

Acknowledgement

This work was supported in part by the National Science Foundation under grant IIP-1362022 and from the WindSTAR I-UCRC Industry Advisory Board. The authors are grateful to Neal Fine and John Cooney from Aquanis for stimulating discussions on active flow control. Any opinions, findings, and conclusions or recommendations expressed in this material are those of the authors and do not necessarily reflect the views of the sponsors.

References

[1] Barlas, T. K., & Van Kuik, G. A. M. (2007). State of the art and prospectives of smart rotor control for wind turbines. In Journal of Physics: Conference Series (Vol. 75, No. 1, p. 012080). IOP Publishing.
[2] Bossanyi, E. A. (2003). Individual blade pitch control for load reduction. Wind Energy: An International Journal for Progress and Applications in Wind Power Conversion Technology, 6(2), 119-128.
[3] Selvam, K., Kanev, S., van Wingerden, J. W., van Engelen, T., & Verhaegen, M. (2009). Feedback–feedforward individual pitch control for wind turbine load reduction. International Journal of Robust and Nonlinear Control: IFAC-Affiliated Journal, 19(1), 72-91.
[4] Barlas, T. K., & van Kuik, G. A. (2010). Review of state of the art in smart rotor control research for wind turbines. Progress in Aerospace Sciences, 46(1), 1-27.
[5] Bak, C., et al. (2013). The DTU 10-MW reference wind turbine. In Danish Wind Power Research 2013.
[6] Jonkman, B., & Jonkman, J. (2016). FAST v8. 16.00 a-bjj. National Renewable Energy Laboratory.
[7] Hansen, M. H., & Henriksen, L. C. (2013). Basic DTU wind energy controller.
[8] Liu, C., Li, Y., Cooney, J. A., Fine, N. E., & Rotea, M. A. (2018, August). NREL Fast Modeling for Blade Load Control with Plasma Actuators. In 2018 IEEE Conference on Control Technology and Applications (CCTA) (pp. 1644-1649). IEEE.
[9] Bir, G. (2008). Multi-blade coordinate transformation and its application to wind turbine analysis. In 46th AIAA aerospace sciences meeting and exhibit (p. 1300).
[10] Lu, Q., Bowyer, R., & Jones, B. L. (2015). Analysis and design of Coleman transform-based individual pitch controllers for wind-turbine load reduction. Wind Energy, 18(8), 1451-1468.
[11] International Electrotechnical Commission. (2005). IEC 61400-1: Wind Turbines–Part 1: Design Requirements.
[12] Hayman, G. (2012). MLife theory manual for version 1.00. National Renewable Energy Laboratory, Golden, CO, 74(75), 106.